Mechanical Properties, Morphological Structure, and Thermal Behavior of Dynamically Photocrosslinked PP/EPDM Blends

Longxiang Tang,[1] Baojun Qu,[1] Xiaofeng Shen[2]

[1]*Department of Polymer Science and Engineering, University of Science and Technology of China, Hefei, Anhui 230026, China*
[2]*Department of Polymer Science and Engineering, School of Chemistry, Anhui University, Hefei, Anhui 230039, China*

Received 6 June 2003; accepted 20 November 2003

ABSTRACT: A dynamically photocrosslinked polypropylene (PP)/ethylene–propylene–diene (EPDM) rubber thermoplastic elastomer was prepared by simultaneously exposing the elastomer to UV light while melt-mixing in the presence of a photoinitiator as well as a crosslinking agent. The effects of dynamic photocrosslinking and blend composition on the mechanical properties, morphological structure, and thermal behavior of PP/EPDM blends were investigated. The results showed that after photocrosslinking, tensile strength, modulus of elasticity, and elongation at break were improved greatly. Moreover, the notched Izod impact strength was obviously enhanced compared with corresponding uncrosslinked blend. Scanning electron microscopy (SEM) morphological analysis showed that for uncrosslinked PP/EPDM blends, the cavitation of EPDM particles was the main toughening mechanism; whereas for dynamically photocrosslinked blends, shear yielding of matrix became the main energy absorption mechanism. The DSC curves showed that for each dynamically photocrosslinked PP/EPDM blend, there was a new smaller melting peak at about 152°C together with a main melting peak at about 166°C. Dynamic mechanical thermal analysis (DMTA) indicated that the compatibility between EPDM and PP was improved by dynamic photocrosslinking. © 2004 Wiley Periodicals, Inc. J Appl Polym Sci 92: 3371–3380, 2004

Key words: polypropylene; rubber; vulcanization; mechanical properties; graft copolymers

INTRODUCTION

Polypropylene (PP) has been widely used in a variety of applications because of its advantages, such as low cost, low density, high softening point, easy processing, as well as outstanding tensile properties. However, its poor impact strength, especially at low temperature, hinders its application as an engineering thermoplastic. To improve PP impact toughness, various elastomers were applied to PP, such as ethylene–propylene rubber (EPR),[1–3] styrene–butadiene–styrene (SBS) copolymer,[4] butyl rubber,[5] and ethylene–propylene–diene rubber (EPDM).[6,7] Among these rubbers, EPDM is considered as one of the most effective impact modifiers for PP. The incorporation of an elastomer into PP, although increasing its impact strength, usually results in deteriorating the tensile strength and modulus. Fortunately, the mechanical properties of a thermoplastic elastomer blend can be further improved by dynamic vulcanization.[8] In recent years, most studies concern the mechanical and physical properties of dynamically vulcanized PP/EPDM blends,[9–11] which are mostly utilized in the plastic industries. Organic peroxide/coagent system, sulfur/accelerator system, and phenolic resin system are commonly used to prepare dynamically vulcanized PP/EPDM blends. However, organic peroxides degrade the PP matrix greatly, leading to the deterioration of mechanical properties. The instability of polysulfide crosslinking and the odor of a sulfur/accelerator system limit its application. Because the considerable concentrations of phenolic resin and accelerator are required for the crosslinking reaction to proceed effectively, the involved compounds negatively affect the impact strength of the resultant blends.[9]

Hillborn et al. studied photocrosslinking of EPDM systematically, which was crosslinked easily under UV exposure.[12,13] Zamotaev et al. reported photocrosslinking of PP, which revealed that the photodegradation of PP could be depressed by the addition of multifunctional monomers.[14]

A novel technology of dynamic photocrosslinking, which combines photocrosslinking with the technology of dynamic vulcanization, was developed in our laboratory.[15] In the present work, the effects of dynamic photocrosslinking on the mechanical proper-

Correspondence to: B. J. Qu (qubj@ustc.edu.cn).
Contract grant sponsor: National Natural Science Foundation of China; contract grant number: 50073022.

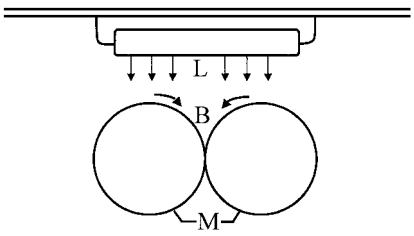

Figure 1 Schematic graph of experimental apparatus. L, B, M represent lamp, blend, and two-roller mixer, respectively.

ties, morphological structure, and thermal behavior of PP/EPDM blends were investigated.

EXPERIMENTAL

Materials

PP [F401, melt flow rate (MFR) = 3.5] was supplied by Yangzi Petrochemical Co. Ltd. (China). EPDM 4045 (60 wt % ethylene, 3 wt % 5-ethylidene-2-norbornene) was supplied by Mitsui Petrochemical Co. Ltd. (Japan). Benzyl dimethyl ketal (BDK), supplied by Jingjiang Chemical Engineering Co. Ltd., (China), was used as a photoinitiator. Triallyl isocyanurate (TAIC) was supplied by Anhui Institute of Chemical Engineering (China) as a crosslinking agent. All materials were used as received without further purification.

Preparation of blends

The uncrosslinked blends were designated as P_mV_0, and the dynamically photocrosslinked blends were designated as P_mV_n, P represents PP; its subscript m denotes the weight percentage of PP in the blends, and the subscript n of V represents UV irradiation time. For example, $P_{70}V_{30}$ indicates 70 wt % PP and 30 wt % EPDM in the blend, which was UV irradiated for 30 s, whereas $P_{70}V_0$ represents uncrosslinked PP/EPDM (70/30) blend. PP was first mixed with a given amount of EPDM, 1 wt % BDK, and 4 wt % TAIC (based on the EPDM content) for 8 min at 180°C by using a two-roller mixer (SK-160B, Shanghai). Then, the melted blend exposed to a 2 kW Philips HPM 15 lamp (80 W/cm) for different times at 7 cm distance from the lamp, while mechanically blending, as shown in Figure 1. After irradiation, the dynamically photocrosslinked blend was continuously mixed for another 5 min. Then, the sample was hot-pressed to sheets of 1- and 4-mm thickness at 200°C and 12 MPa pressure for 5 min by using a press. The appropriate test specimens were cut from the molded sheets.

Measurements

The gel content was measured for the samples after irradiation according to the literature.[16] However, to characterize the crosslinking reaction of EPDM, the degree of crosslinking was calculated by using the equations:

$$\text{Gel content (\%)} = \frac{\text{sample weight after extraction}}{\text{sample weight before extraction}} \times 100$$

$$\text{Degree of crosslinking (\%)} = \frac{\text{gel content}}{\text{wt \% of elastomer in the blend}} \times 100$$

The MFR was determined at 230°C under a load of 2.16 kg according to ASTM D-1238 standard.

Tensile properties were measured on an Instron universal tester (model 1185) at 25 ± 2°C with dumbbell-shaped specimens at a crosshead speed of 25 mm/min, with an initial gauge length of 25 mm. Tensile strength (TS), tensile stress at break (TS_b), tensile stress at yield (TS_y), tensile stress at 100% elongation ($TS_{100\%}$), modulus of elasticity (E_t), and elongation at break (E_b) were recorded. The notched Izod impact strength (Notched-IIS) was carried out by using an Izod impact tester (Chengde Precise Tester To., Ltd., China) at 23 and −30°C. The samples with a size of 80 × 10 × 4 mm^3 and a single-edge 45° V-shaped notch (tip radius, 0.25 mm; depth, 2 mm) were used. The average value from five specimens for each composition was reported.

The phase structures of the blends were analyzed by a scanning electron microscope (SEM; Hitachi X560 scanning electron microanalyzer, Japan). The uncrosslinked and dynamically photocrosslinked PP/EPDM blends were impact fractured (at room temperature) and cryogenically fractured (in liquid nitrogen). To observe the fracture morphology change, EPDM was selectively etched by using xylene at 23°C for 10 min in an ultrasonic cleaner, and the surface was coated with a conductive gold layer.

A Perkin–Elmer DSC-2 instrument was used to investigate the crystallization and melting behavior of the blends. To prevent the samples from thermal oxidation, all measurements were carried out in a nitrogen atmosphere. All samples were approximately 10 mg in weight. Each sample was analyzed in the following manner:

1. The sample was placed in the sample cell, heated to 200°C at a heating rate of 60°C/min, and held for 5 min to eliminate previous thermal history.

2. The sample was then cooled from 200 to 60°C at a cooling rate of 20°C/min and held for 3 min (crystallization).

TABLE I
Tensile Properties of the PP/EPDM Blends

Blend system	Sample code	TS	TS_b	TS_y	$TS_{100\%}$	E_1	E_b (%)
		(MP_a)					
Uncrosslinked blends	$P_{90}V_0$	28.9 ± 1.2	31.3 ± 1.3	27.2 ± 1.0	27.9 ± 1.1	763 ± 33	550 ± 22
	$P_{80}V_0$	20.7 ± 0.9	21.2 ± 1.0	20.0 ± 0.9	20.7 ± 0.7	668 ± 28	440 ± 20
	$P_{70}V_0$	17.3 ± 0.7	16.9 ± 0.8	16.4 ± 0.7	16.9 ± 0.5	363 ± 16	400 ± 17
	$P_{60}V_0$	12.4 ± 0.4	12.0 ± 0.5	11.3 ± 0.4	12.4 ± 0.3	243 ± 11	320 ± 14
	$P_{50}V_0$	8.9 ± 0.5	8.6 ± 0.4	8.2 ± 0.5	8.9 ± 0.3	154 ± 6	230 ± 9
Photocrosslinked blends	$P_{90}V_{60}$	34.2 ± 1.4	33.1 ± 1.4	27.1 ± 1.2	34.2 ± 1.4	1070 ± 42	760 ± 31
	$P_{80}V_{60}$	26.0 ± 1.2	22.1 ± 1.2	18.9 ± 1.0	26.0 ± 1.1	709 ± 31	930 ± 40
	$P_{70}V_{60}$	21.2 ± 0.8	18.8 ± 1.0	17.5 ± 0.8	20.2 ± 0.9	631 ± 26	640 ± 28
	$P_{60}V_{60}$	18.2 ± 0.6	17.3 ± 0.7	15.7 ± 0.8	18.2 ± 0.5	473 ± 17	500 ± 22
	$P_{50}V_{60}$	16.3 ± 0.7	15.5 ± 0.7	14.6 ± 0.4	16.0 ± 0.6	276 ± 11	330 ± 13
PP/EPDM (70/30) blends	$P_{70}V_0$	17.3 ± 0.7	16.9 ± 0.8	16.4 ± 0.7	16.9 ± 0.5	363 ± 16	400 ± 17
	$P_{70}V_{15}$	17.7 ± 0.8	17.3 ± 0.6	16.2 ± 0.5	17.7 ± 0.7	413 ± 19	520 ± 22
	$P_{70}V_{30}$	19.9 ± 1.0	17.9 ± 0.8	16.6 ± 0.3	18.9 ± 0.9	545 ± 23	580 ± 20
	$P_{70}V_{60}$	21.2 ± 0.8	18.8 ± 1.0	17.5 ± 0.8	20.2 ± 0.9	631 ± 26	640 ± 28
	$P_{70}V_{120}$	17.3 ± 0.7	17.1 ± 1.0	16.6 ± 0.7	17.3 ± 0.6	359 ± 16	270 ± 13

3. Finally, the sample was immediately heated from 60 to 200°C at 20°C/min (melting).

The crystallization temperature, melting temperature, and the enthalpy of fusion of the blends were obtained. The crystallinity X_c was calculated by the relative ratio of the enthalpy of fusion per gram of the blend to the heat of fusion of PP crystal (209 J/g).[17]

The dynamic mechanical properties were evaluated by using a dynamic mechanical thermal analyzer (DMTA) IV (Rheometric Scientific Co. Ltd., USA). The compression-molded sample size was 30 × 8 × 1 mm^3. Testing was carried out in a temperature range of −100 to 100°C at a constant frequency of 5 Hz and a heating rate of 5 K/min. The temperature dependence on the loss tangent (tan δ) was recorded.

RESULTS AND DISCUSSION

Mechanical properties

The tensile properties of uncrosslinked and dynamically photocrosslinked PP/EPDM blends are summarized in Table I. For both uncrosslinked and dynamically photocrosslinked PP/EPDM blends, TS, TS_b, TS_y, $TS_{100\%}$, E_t, and E_b decreased as the EPDM content increased. The reduction in tensile properties can be expected as the result of the rubbery nature of EPDM and thus lowers the crystallinity of blends in relation to pure PP. However, in comparison with uncrosslinked PP/EPDM blends, corresponding dynamically photocrosslinked PP/EPDM blends displayed higher TS, E_t, and E_b. Moreover, these tensile properties increased with increasing radiation time except for 120 s. The increase of E_t is attributed to the crosslinking of rubbery phase, whereas the improvement of TS and E_b is due to the enhanced interfacial adhesion resulting from dynamic photocrosslinking,[18] which causes efficient stress transfer between the matrix and the dispersed phase, and consequently, suppresses the generation of voids or flaws in PP matrix. However, when irradiated for 120 s, the significant decreases of all tensile properties were observed as compared with those for 60 s irradiation. This is attributed to the photodegradation of PP as a main reaction, leading to low molecular weight and consequently deterioration of tensile properties.[19] It has been also found that the $P_{80}V_{60}$ blend showed the maximum elongation at break, which may be interpreted as due to a number of factors acting independently and simultaneously, including the decrease of crystallinity of PP resulting from blending with EPDM, the photodegradation of PP, and the photocrosslinking of EPDM, etc.

Table II lists the Notched-IIS of uncrosslinked and

TABLE II
Effects of Photocrosslinking and Composition on the Impact Strength of PP/EPDM Blends

Sample code	MFR (g/10 min)	Degree of crosslinking (%)	Notched-IIS (kJ/m^2)	
			25°C	−30°C
$P_{90}V_0$	3.2	—	11.6 ± 0.6	4.7 ± 0.2
$P_{90}V_{60}$	3.8	27.0	16.4 ± 0.7	6.7 ± 0.2
$P_{80}V_0$	2.8	—	19.5 ± 0.9	8.8 ± 0.4
$P_{80}V_{60}$	3.0	41.0	35.2 ± 1.4	13.7 ± 0.5
$P_{70}V_0$	2.1	—	34.9 ± 1.4	9.7 ± 0.4
$P_{70}V_{15}$	1.6	9.7	37.5 ± 1.6	10.3 ± 0.4
$P_{70}V_{30}$	1.9	29.7	48.7 ± 2.2	11.6 ± 0.6
$P_{70}V_{60}$	2.2	55.0	66.3 ± 3.0	16.1 ± 0.9
$P_{70}V_{120}$	3.5	62.0	43.4 ± 1.9	10.6 ± 0.4
$P_{60}V_0$	1.3	—	41.7 ± 1.7	19.0 ± 0.7
$P_{60}V_{60}$	1.9	71.8	69.1 ± 2.8	21.9 ± 0.9
$P_{50}V_0$	1.1	—	39.9 ± 1.3	24.1 ± 1.1
$P_{50}V_{60}$	1.7	76.8	70.5 ± 3.2	28.3 ± 1.3

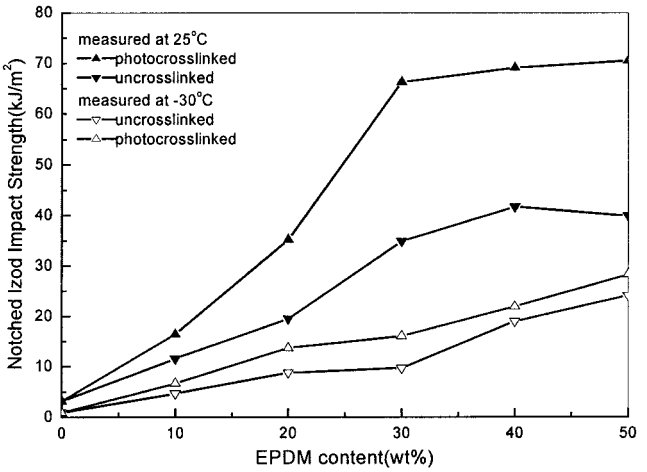

Figure 2 Notched-IIS versus EPDM content of uncrosslinked and dynamically photocrosslinked PP/EPDM blends measured at 25 and −30°C.

dynamically photocrosslinked PP/EPDM blends containing different contents of EPDM measured at 23 and −30°C. As can be seen in Table II, both MFRs of uncrosslinked and dynamically photocrosslinked blends gradually decreased with increasing the rubber weight percentage in the blend. In comparison with uncrosslinked PP/EPDM blends, however, dynamically photocrosslinked PP/EPDM blends displayed higher MFRs, which is ascribed to the dispersed smaller EPDM particles in PP matrix and the photodegradation of PP. As we know, the termed MFR is a measure of the ability of a material to flow. Therefore, the increase of MFR of the dynamically photocrosslinked PP/EPDM blends implies a better processing property compared with corresponding uncrosslinked blends. Moreover, the degree of crosslinking increased with increasing EPDM content in the blend and dynamic photocrosslinking time (Table II).

Figure 2 shows the variation of Notched-IIS of PP/EPDM blends with EPDM contents measured at 25 and −30°C. The data are listed in Table II. For uncrosslinked samples, the impact strength increased gradually from 3.2 kJ/m^2 of PP to 41.7 kJ/m^2 of the blend containing 40 wt % EPDM; while further increasing the EPDM content to 50 wt %, a slight decrease of the impact strength can be observed. However, after dynamic photocrosslinking, the quite sharp rise of the impact strength from 3.2 kJ/m^2 of PP to 66.3 kJ/m^2 of the blend containing 30 wt % EPDM rubber was obtained. After increasing the EPDM content from 30 to 50 wt % in the blend, the impact strength was leveled off. Therefore, the addition of 30 wt % EPDM in a blend is most recommended for balancing the impact toughness and tensile strength.

Although at −30°C, a gradual increase of impact strength was obtained with increasing EPDM content, a relatively lower impact strength was observed compared with those of both dynamically photocrosslinked and uncrosslinked blends at 25°C. This is due to the higher glass transition temperature (T_g, 13°C) of PP, which leads to its brittle behavior at −30°C, and thus, difficult deformation of PP matrix. However, the shear yielding of the matrix is important, because it is considered to be the main impact energy absorption mechanism.[20,21]

The effects of dynamic photocrosslinking times on the impact strength of the PP/EPDM (70/30) blend are given in Figure 3. The data are also listed in Table II. At 25°C, the impact strength of the blend increases sharply with an increase in the dynamic photocrosslinking time up to 60 s and then decreases markedly when further prolonging the dynamic photocrosslinking time. At −30°C, the impact strength shows a similar trend with that at 25°C. It is probably due to the existence of two competing reactions: photocrosslinking of EPDM particles and photodegradation of PP matrix. The photocrosslinking of EPDM component for the blends dynamically photocrosslinked for less than 60 s is predominant. It is assumed that the compatibility between PP and EPDM was improved by the obtained graft copolymer of PP and EPDM, leading to the dramatic increase of impact strength of the PP/EPDM blend. However, as the dynamic photocrosslinking time exceeded 60 s, the photodegradation of PP was the major reaction, resulting in the decrease of molecular weight and thus in the impact strength of PP/EPDM blends.

Morphological structure

The SEM micrographs of fracture surfaces of cryofractured samples and their etched samples in xylene to dissolve out EPDM component are shown in Figure 4 for uncrosslinked [Fig. 4(a–e)] and dynamically pho-

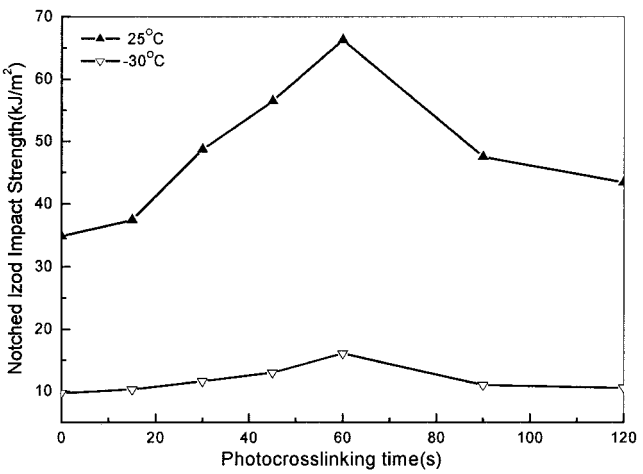

Figure 3 Notched-IIS versus photocrosslinking time for PP/EPDM (70/30) measured at 25 and −30°C.

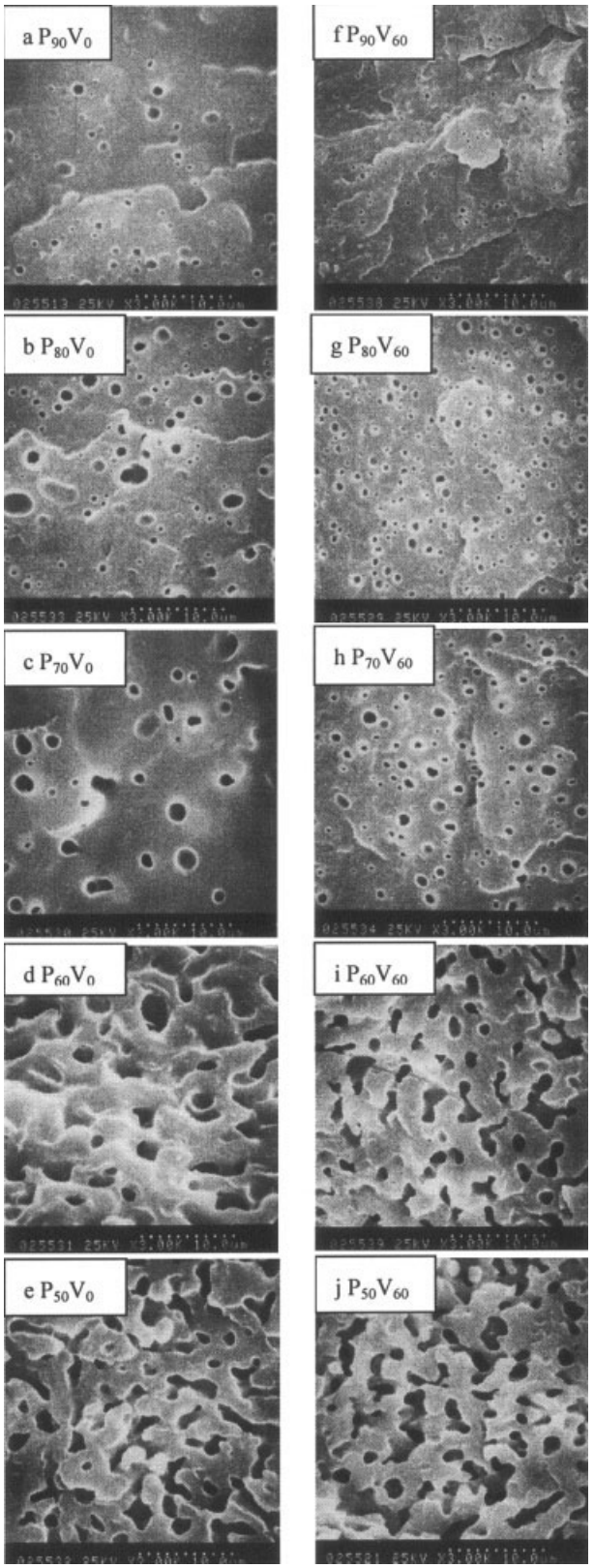

Figure 4 SEM images of cryofractured and etched surfaces of uncrosslinked and dynamically photocrosslinked PP/EPDM blends.

tocrosslinked samples containing different EPDM contents [Fig. 4(f–j)]. The holes indicate the sites where the rubber particles are located prior to etching. It can be observed that the two-phase morphology exists in all systems, which indicates the immiscibility of PP and EPDM in the blends. However, for uncrosslinked blends, with increasing the rubber content to 30 wt % in the blend, the rubber particle size increases considerably, which can be ascribed to the reagglomeration or the coalescence of dispersed rubber particles.[22,23] In these blends, PP is obviously a continuous phase. However, as EPDM content is up to 50 wt %, EPDM phase and PP matrix form a cocontinuous morphology, which can be considered as a three-dimensional (3D) structure that consists of elongated domains and is interconnected. The similar phenomenon was observed in literature.[24] In a word, for uncrosslinked blends, because of the deficiency of interfacial adhesion between two phases, the morphology is quite rough, and the EPDM particles are distributed coarsely in the PP matrix.

In comparison with the morphology of uncrosslinked PP/EPDM blends, the dynamically photocrosslinked EPDM are finely dispersed in very small particles in the PP matrix and the number density of the dispersed rubber domains is higher. The larger the number of potential craze initiators (i.e., elastomer particles), the higher impact strength of vulcanized blends can be obtained.

To investigate the deformation-induced changes during Izod test at room temperature, the fracture surfaces of PP and PP/EPDM blends etched in xylene were observed by using SEM, as shown in Figure 5. The fracture surface of PP appears relatively smooth, indicating that little plastic deformation has taken place during the impact test. For uncrosslinked blends containing 20 wt % EPDM content, it can be observed that there seems to be no evidence of adhesion between the dispersed phase and the matrix. It is well known that cavitation is associated with debonding of rubber particles from the matrix, which dissipates less energy than shear yielding, resulting in the lower impact strength of a blend. However, for the dynamically photocrosslinked blends with addition of 10–20 wt % EPDM, more and smaller voids were observed [Fig. 5(f, g)]. Moreover, some voids were elongated, which are formed as a result of plastic deformation surrounding the matrix.[25] This suggests that during the brittle fracture, the rubber cavitations are taking place; the matrix shear yielding in-between the cavities is, however, also present, which dissipates much more energy in the matrix than the cavitations. Consequently, the dynamically photocrosslinked blends display higher impact strength than that of uncrosslinked blends. For such blends, two mechanisms of energy absorption coexist, namely by cavitation and shear yielding. As we know, matrix shear yielding is

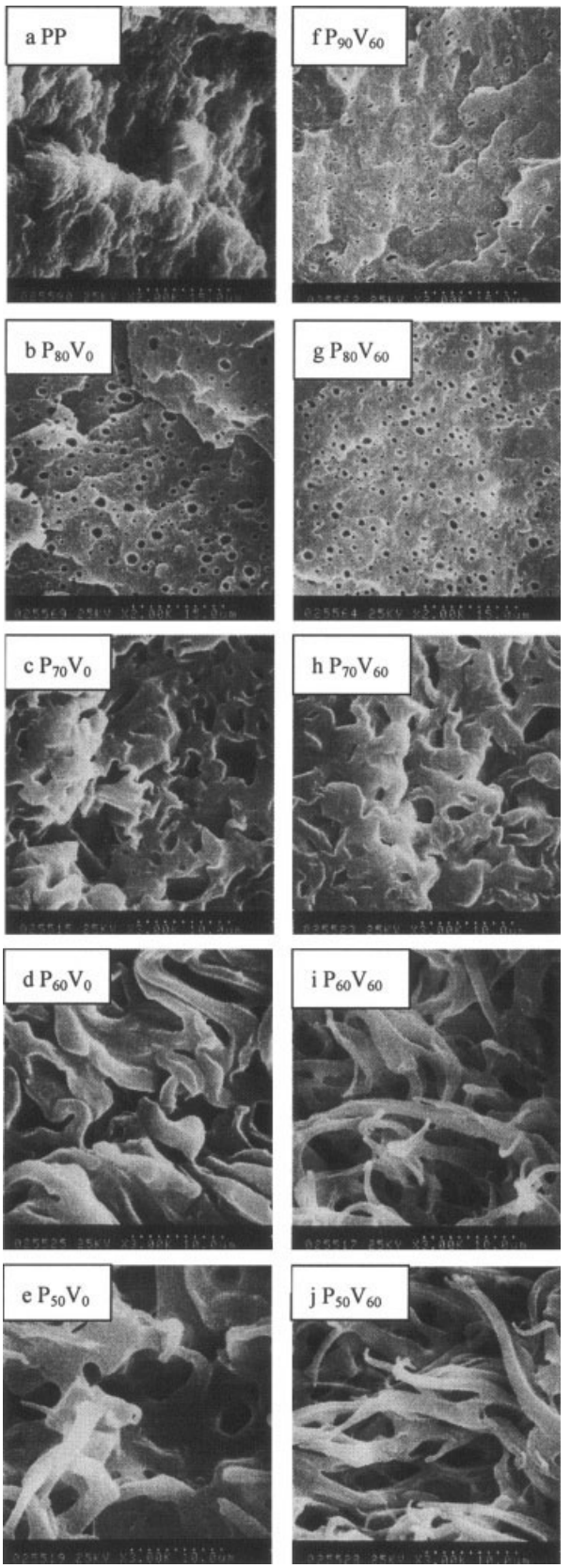

Figure 5 SEM images of fractured and etched surfaces of uncrosslinked and dynamically photocrosslinked PP/EPDM blends after Izod impact test at 25°C.

considered to be the main energy absorption mechanism.[20,21]

As EPDM content in the dynamically photocrosslinked blends increases to 30–50 wt %, the fracture surfaces of these blends show extensive plastic deformation of the matrix [Fig. 5(h–j)]. The formation of massive striations on fracture surfaces indicates massive shear yielding in the matrix. However, in the case of uncrosslinked blends, there was no massive plastic deformation because the stress concentration zone was not continuous. It is evidence for improving impact strength by dynamic photocrosslinking. In a word, for the uncrosslinked blends with 30–50 wt % EPDM, the impact energy is dissipated by both cavitation and shear yielding, whereas for the dynamically photocrosslinked blends with 30–50 wt % EPDM, the matrix shear yielding becomes the main energy absorption mechanism. The change of morphological features after dynamic photocrosslinking is attributed to the enhancement of compatibility between EPDM particles and PP matrix, which is important that the stress concentration fields developed from the EPDM particles interact effectively with each other in PP matrix. If the interface between the EPDM particles and the matrix debonds during the deformation before the interaction is attained, voids or flaws are produced. On the other hand, if the sufficient interaction is attained, a continuous stress concentration zone is realized in the matrix and the blend. This enables shear yielding to occur easily and as a result, the energy absorption in these blends will increase dramatically.

Thermal behavior

The thermal properties of PP and PP/EPDM blends are listed in Table III. It is obvious that for both uncrosslinked and dynamically photocrosslinked PP/EPDM blends, the melting transition of PP shows little or no change (only a few degrees) with the addition of EPDM. Their crystallization temperatures also remain virtually constant with increasing EPDM content. However, the heat of fusion and the crystallinity of both series of PP/EPDM blends decrease with increasing the EPDM content, which is due to the dilution effect of EPDM. In comparison with uncrosslinked blends, corresponding dynamically photocrosslinked blends show lower crystallinity, which is attributed to the enhancement of compatibility, leading to more entanglement of chains restricting the crystallization of PP and consequently forming more imperfect crystals of PP.

The effects of dynamic photocrosslinking time on the crystallization and melting behaviors of PP/EPDM (70/30) blend are also given in Table III. It can be found that there are no significant changes in the melting and crystallization temperatures for the

TABLE III
Crystallization and Melting Behaviors of PP/EPDM Blends

Blend system	Sample code	Heat of fusion (ΔH), J/g	Melting temperature (T_m), °C	Crystallization temperature (T_c), °C	Crystallinity (%)
Uncrosslinked blends	PP	86.6	166.7	107.4	41.4
	$P_{90}V_0$	84.6	167.1	112.0	40.5
	$P_{80}V_0$	74.6	168.1	105.8	35.7
	$P_{70}V_0$	67.5	166.9	108.5	32.3
	$P_{60}V_0$	52.4	166.5	107.3	25.0
	$P_{50}V_0$	43.0	166.9	107.5	20.6
Photocrosslinked blends	$P_{90}V_{60}$	83.1	169.8	108.0	39.8
	$P_{80}V_{60}$	72.4	166.1	107.4	34.6
	$P_{70}V_{15}$	60.7	165.2	107.5	29.0
	$P_{70}V_{30}$	59.8	167.3	108.4	28.6
	$P_{70}V_{60}$	57.9	164.9	108.0	27.7
	$P_{70}V_{120}$	56.4	165.8	107.7	27.0
	$P_{60}V_{60}$	51.6	168.1	105.0	27.7
	$P_{50}V_{60}$	35.8	167.1	107.7	17.1

blends dynamically photocrosslinked for different times. The slight decrease in their crystallinity is probably due to the enhanced compatibility, resulting in favorable entanglements of chains and thus imperfect crystals of PP.

The melting behavior of PP and uncrosslinked PP/EPDM blends are shown in Figure 6. There is no evident difference in the feature of melting curves, while the decreased area of the endothermic peak with increasing EPDM content can be observed. Moreover, it has been found from Figures 7 and 8 that a new smaller melting peak emerges at about 152°C besides a main melting peak at the melting curves for all dynamically photocrosslinked PP/EPDM blends and becomes larger with increasing the dynamic photocrosslinking time. Those smaller melting peaks are probably assigned to the graft copolymers of PP and EPDM, such as PP-EPDM or PP-TAIC-EPDM at the interface.[15]

The glass transition behavior of a polymer blend is strongly governed by the interaction between its components. In other words, the behavior is directly affected by the compatibility of components in a blend. As we know, there exists only one glass transition in a compatible blend, whereas more than one glass transition corresponds to its components in an incompatible blend. Moreover, for a partially compatible system, the glass transition temperatures of its components will shift inward, and the extent of inward shifting indicates the level of the compatibility of the components.[26] In this work, the glass transition behavior and compatibility of uncrosslinked and dynamically photocrosslinked PP/EPDM blends were investigated by using DMTA technique. The effects of dynamic photocrosslinking and blend composition on the tan δ of the samples are given in Figure 9 and the

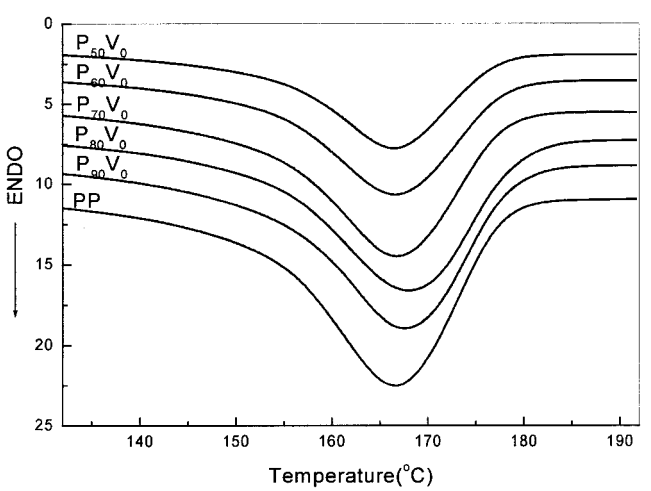

Figure 6 Melting behavior of PP and uncrosslinked PP/EPDM blends.

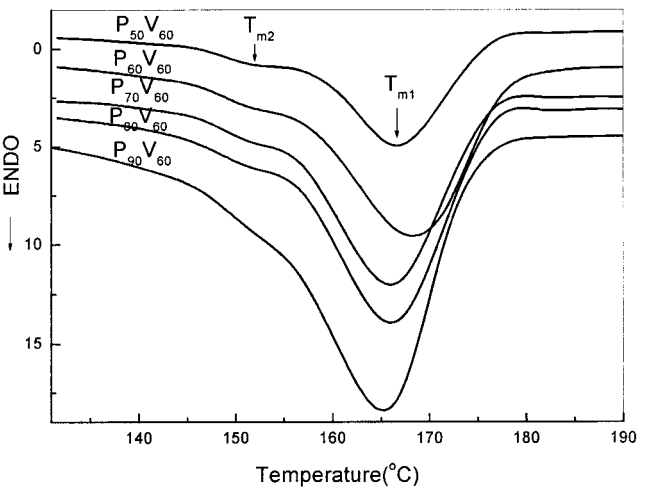

Figure 7 Melting behavior of dynamically photocrosslinked PP/EPDM blends.

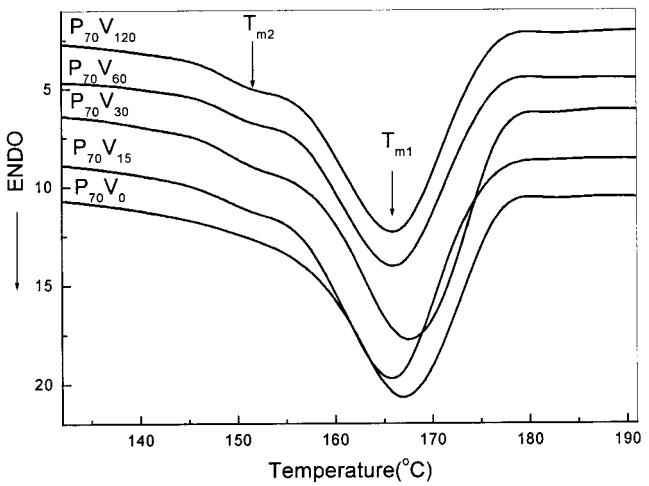

Figure 8 Melting behavior of PP/EPDM (70/30) blend dynamically photocrosslinked for different times.

transition temperatures (T_g) are listed in Table IV. It is not surprising that two main relaxation regions exist for both uncrosslinked and dynamically photocrosslinked samples. These separated peaks for the individual components indicate the incompatible nature of the blends, which is consistent with the microscopic observations. The transition around −56°C is attributed to EPDM component, and its relative magnitude increases with the increase of EPDM content, whereas the relaxation region around 13°C is attributed to PP component, and its relative magnitude decreases with increasing EPDM content. From Table IV, it was found that the positions of both peaks for the uncrosslinked blends are almost unchanged; thus, it can be deduced that there is no significant interaction between PP and EPDM. However, after dynamic photocrosslinking, the T_g peaks for EPDM at all content shift upward, whereas the T_g peaks for PP shift to

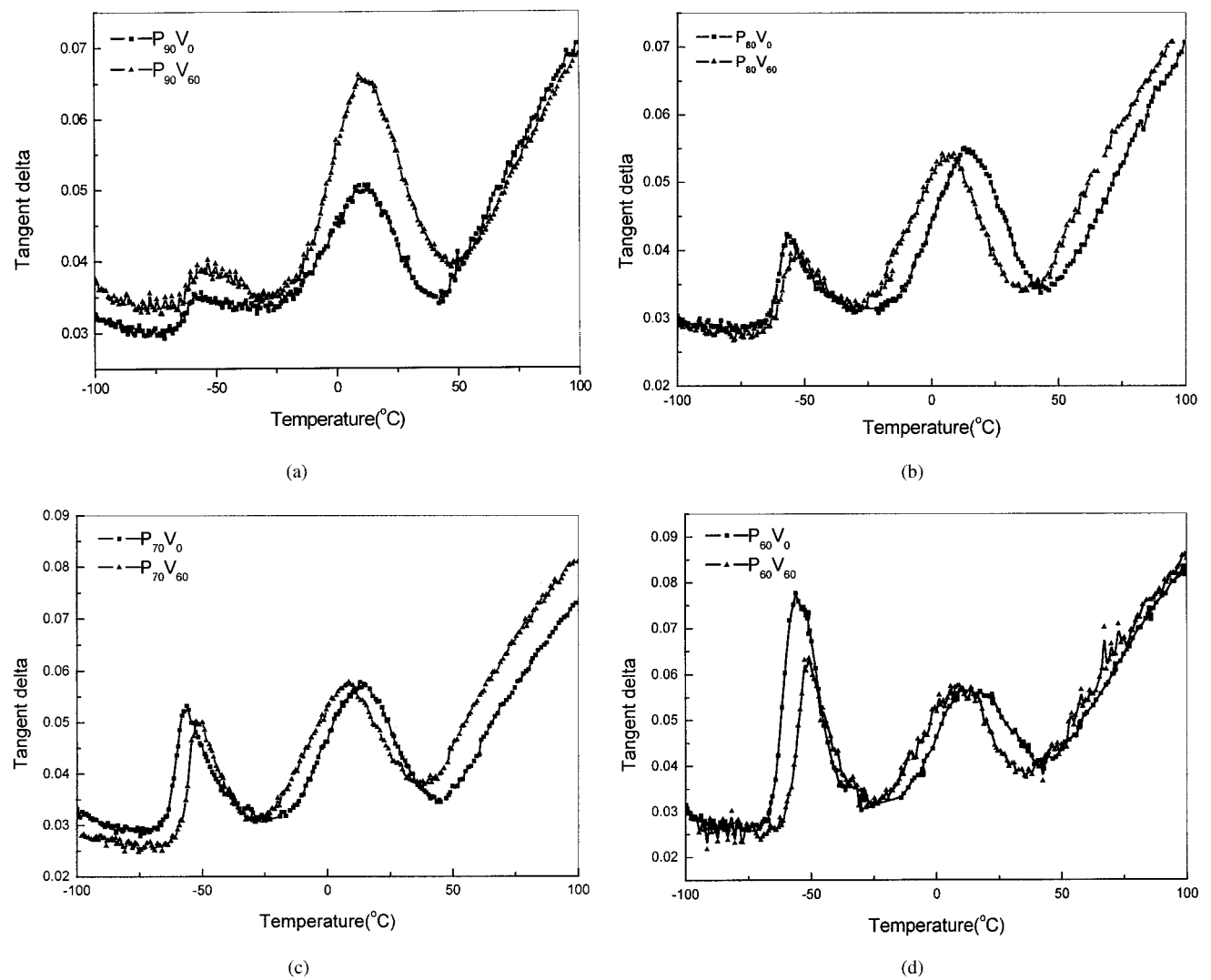

Figure 9 Loss tangent (tan δ) as a function of temperature at 5 Hz for uncrosslinked and dynamically photocrosslinked PP/EPDM blends with different compositions.

lower temperatures. As a result, the extent of inward shifting amounts to 8.9°C for $P_{60}V_{60}$ compared with the uncrosslinked $P_{60}V_0$ blend. Because the extent of inward shifting is considered to be a parameter indicating the compatibility of EPDM particles with PP matrix, it can be deduced that dynamic photocrosslinking promotes interfacial bonding between the phases, resulting in the massive shear yielding of PP matrix and thus the higher impact strength (Fig. 2).

Figure 10 shows the effects of dynamic photocrosslinking time on the tan δ of PP/EPDM (70/30) blends. It is evident that the extent of inward shifting increases with increasing the dynamic photocrosslinking time, which is probably due to the production of a larger number of grafted chains of PP and EPDM. However, as shown in Figure 3, when dynamic photocrosslinking time exceeded 60 s, the impact strength of the blend began to decrease, which is probably due to the photodegradation of PP matrix. Therefore, the improvement of the extent of inward shifting does not correspond to the improvement of interfacial adhesion and impact strength. There are other factors except for the enlargement of the extent of inward shifting, such as the increase of T_g of EPDM resulting from photocrosslinking. According to Flory's free-volume theory, the end groups possess higher mobility than other parts in molecular chains. When PP is photodegraded, the proportion of end groups increases and thus some chain units can move at relatively lower temperature, resulting in the decrease of T_g of PP. Therefore, photodegradation of PP also probably contributes to the extent of inward shifting of T_g of PP, which, together with the effect of UV exposure on the thermal behavior and mechanical properties of neat PP, has been systematically investigated in the literature.[27]

TABLE IV
Glass Transition Temperatures of PP and EPDM in PP/EPDM Blends

Sample code	T_{g1} (°C)	T_{g2} (°C)	ΔT_g ($T_{g2}-T_{g1}$)[a] (°C)	Extent of inward shifting[b] (°C)
$P_{90}V_0$	−56.3	13.1	69.4	—
$P_{90}V_{60}$	−53.3	9.1	62.4	7.0
$P_{80}V_0$	−57.0	13.0	70.0	—
$P_{80}V_{60}$	−53.1	8.7	61.8	8.2
$P_{70}V_0$	−56.3	13.0	69.3	—
$P_{70}V_{15}$	−54.4	9.3	63.7	5.6
$P_{70}V_{30}$	−53.3	9.1	62.4	6.9
$P_{70}V_{60}$	−52.5	8.5	61.0	8.3
$P_{70}V_{120}$	−51.5	7.0	58.5	10.8
$P_{60}V_0$	−56.1	12.8	68.9	—
$P_{60}V_{60}$	−50.8	9.2	60.0	8.9

[a] T_{g1} and T_{g2} represent T_g of EPDM and PP components in the blends, respectively.

[b] Extent of inward shifting = ΔT_g of dynamically photocrosslinked PP/EPDM blends—ΔT_g of corresponding uncrosslinked blends.

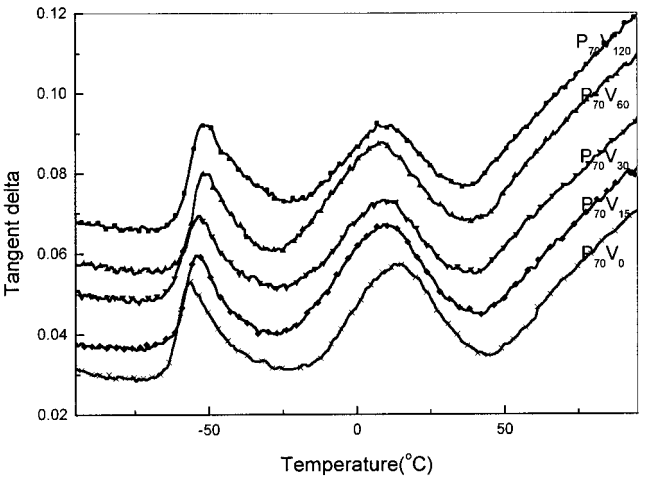

Figure 10 tan δ as a function of temperature at 5 Hz for PP/EPDM (70/30) blends dynamically photocrosslinked for different times.

CONCLUSION

This study reveals the positive influence of the blend composition and dynamic photocrosslinking on the mechanical properties, morphological structure, and thermal behavior of PP/EPDM blends. For dynamically photocrosslinked PP/EPDM blends, due to the improvement of compatibility between PP and EPDM, the increasing interfacial adhesion permits the interaction of stress concentration zone developed from the elastomer particles under deformation and promotes the shear yielding in PP matrix. Therefore, the impact energy dissipation is mainly through shear yielding of the matrix; as a result, the impact strength of blends was enhanced dramatically. DSC thermal analysis showed that grafted chains of PP and EPDM probably existed in the dynamically photocrosslinked blends. DMTA showed that dynamic photocrosslinking could evidently enhance the compatibility between EPDM and PP.

References

1. D'orazio, L.; Greco, R.; Mancarella, C.; Martuscelli, E.; Ragosta, G.; Silvestre, C. Polym Eng Sci 1982, 22, 536.
2. Jancar, J.; DiAnselmo, A.; DiBenedetto, A. T.; Kucera, J. Polymer 1993, 34, 1684.
3. Yokoyama, Y.; Ricco, T. Polymer 1998, 39, 3675.
4. Choudhary, V.; Varma, H. S.; Varma, I. K. Polymer 1991, 32, 2534.
5. Liao, F. S.; Su, A. C. Polymer 1994, 35, 2579.
6. Wang, C.; Chang, C. I. J Appl Polym Sci 2000, 75, 1033.
7. Wal, A. V. D.; Mulder, J. J.; Oderkerk, J.; Gaymans, R. J. Polymer 1998, 39, 6781.
8. Dao, K. C. Polymer 1984, 25, 1527.
9. Inoue, T. J Appl Polym Sci 1994, 54, 709–710.
10. Gupta, N. K.; Jain, A. K.; Singhal, R.; Nagpal, A. K. J Appl Polym Sci 2000, 78, 2104.
11. Ha, C. S.; Ihm, D. J.; Kim, S. C. J Appl Polym Sci 1986, 32, 6281.

12. Hilborn, J.; Rånby, B. Rubber Chem Technol 1988, 61, 568.
13. Hilborn, J.; Rånby, B. Rubber Chem Technol 1989, 62, 592.
14. Zamotaev, P.; Shibirin, E.; Nogellova, Z. Polym Degrad Stab 1995, 47, 93.
15. Wang, W. Z.; Wu, Q. H.; Qu, B. J. Polym Eng Sci to appear.
16. Qu, B.; J.; Rånby, B. J Appl Polym Sci 1993, 48, 703.
17. Silva, A. L. N.; Coutinho, F. M. B.; Rocha M. C. G.; Travares M. I. B. J Appl Polym Sci 1997, 66, 2005.
18. Kimberly, A. C.; Frank, S. B.; Patrick, B. J Appl Polym Sci 2000, 38, 109.
19. Lazar, M.; Rado, R.; Rychly, J. Adv Polym Sci 1990, 95, 149.
20. Wu, S. J Polym Sci, Part B: Polym Phys 1983, 21, 699.
21. Li, Q.; Zheng, W. G.; Qi, Z. N. Sci China (Ser B) 1993, 36, 1305.
22. Martuscelli, E.; Liva, F.; Sellitti, C. Polymer 1985, 26, 117.
23. Thomas, S.; Gupta, B. K.; De, S. K. J Vinyl Technol 1987, 2, 7.
24. Veenstra, H.; Van, D. J.; Dosthuma, A. D. B. Polymer 1999, 40, 1119.
25. Wal, A. V. D.; Gaymans, R. J. Polymer 1999, 40, 6067.
26. Olabisi, O.; Robeson, L. M.; Shaw, M. F. Polymer-Polymer Miscibility; Academic Press: New York, 1979.
27. Tang, L. X.; Wu, Q. H.; Qu, B. J. Polym Degrad Stab to appear.